Magnesium Aluminate Spinel Material Structure and Surface Morphology

[1] Soe Soe Oo, [2] Zaw Win, [3] Hla Hla Win*
[1] Technological University (Yamethin), Yamethin, Myanmar
[2] Technological University (Mandalay), Mandalay, Myanmar
[3] Myanmar Aerospace Engineering University, Meiktila, Myanmar
drsoesoeoo2016@gmail.com, drzawwin2015@gmail.com

***Abstract*— The structural and surface morphological properties of $MgAl_2O_4$ spinel were determined by using X-ray Diffraction (XRD) and Scanning Electron Micrographs (SEM) techniques. From self-heat-sustained method, the results revealed that the samples consisted entirely of well nano-crystalline spinel $MgAl_2O_4$ particles depending upon XRD data. X-ray diffraction analysis confirmed the formation of crystallite sizes and lattice constant in the powders having a single phase cubic structure. The crystallite sizes of the samples at various temperatures have been compared from measured data and the Scherrer calculation. The grain sizes of samples have been studied by SEM. The powder sample ($MgAl_2O_4$ at 800 °C) should be used to get high performance device as the grain sizes are small and homogeneous than other higher temperatures.**

***Keywords*— X-ray Diffraction, Scanning Electron Micrographs, $MgAl_2O_4$, Scherrer calculation, grain size**

I. INTRODUCTION

The magnesium aluminate, $MgAl_2O_4$ crystals present spinel structure, thus a lot of important properties used in industrial applications. Magnesium aluminate spinel is an excellent refractory oxide of immense technological importance as a structural ceramic. It possesses useful physical, chemical and thermal properties, both at normal and elevated temperatures. Magnesium aluminium spinel ($MgAl_2O_4$) has attracted a great deal of attention as a technologically important advanced ceramic material owing to its high melting point. It shows high resistance to attack by most of the acids and alkalis and has low electrical losses. With the aim of increasing the extent of spinellization, lowering the temperature of calcination, and enhancing the densification in the calcinated bodies under less demanding conditions, synthesis of the $MgAl_2O_4$ via self-heat-sustained (SHS) technique was employed.

$MgAl_2O_4$ finds applications ranging from traditional refractories to some advanced usage like infrared and humidity sensors, armour materials, excellent transparent material for arc-enclosing envelopes and alkali-metal vapour discharge devices. The sample requires calcination of the amorphous product at high temperature to yield a perfect single-phase spinel. The calcination, if done at different temperatures, may involve some alteration in phases present, relative amount of phases and (dis)order in spinel structure. The present research work also describes the formation and estimation of the disordered spinel phase, which is chemically induced. Spinels are a special class of crystal structure (AB_2O_4) in which $MgAl_2O_4$ is the more common member having wide commercial applications. The degree of disorder may change with calcinations temperature. In the present study, $MgAl_2O_4$ has been synthesized by using $Mg(OH)_2$ and metallic Al_2O_3 powders. They were accurately weighed and thoroughly mixed with molar ratio in an agate mortar to give about 30 g of the mixed powder. Self-ignition of the gel-like mass crystallized to Mg-Al spinel on calcination at temperatures 700 ˚C to 900 ˚C. X-ray diffraction studies were carried out to study the phase evolution and disorder in spinel phase. And surface morphologies of $MgAl_2O_4$ were observed by using Scanning Electron Microscope.

II. FUNDAMENTAL OF MATERIALS CHARACTERIZATION

A. X-ray Diffraction (XRD)

X-ray diffraction (XRD) is a powerful technique. It is the most widely used for the identification of unknown crystalline materials (eg- minerals, inorganic compounds). Other applications are the characterization of crystalline materials, identification of fine-grained materials such as clays and mixed layer clays that are difficult to determine optically, determination of unit cell dimensions and measurement of sample purity. XRD is also used to determine the thickness of thin films and multilayer and atomic arrangements in amorphous materials (including polymers) and at interfaces.

The specific wavelengths are characteristic of the target material (Cu, Fe, Mo, Cr). Copper is the most common target material for single-crystal diffraction, with CuK_α radiation. Filtering by foils or crystal monochromators, is required to produce monochromatic X-rays needed for diffraction. These X-rays are collimated and directed onto the sample. As the sample and detector are rotated, the intensity of the reflected X-ray is recorded.

When the geometry of the incident X-rays impinging the sample satisfies the Bragg equation, constructive interference occurs and peak intensity occurs. A detector records and processes this X-ray signal and converts the signal to a count rate which is then output to a device such as a printer or computer monitor. The geometry of an X-ray diffractrometer is such as the sample rotates in the path of the collimated X-ray beam at an arm to collect the diffracted X-rays and rotates at an angle of 2θ. The instrument used to maintain the angle and rotate the sample is termed a goniometer. Figure 1 shows the basic features of an XRD experiment set up of the diffraction angle 2θ is the angle between the incident and diffracted X-rays. From 2θ values for reflection, 'd_{hkl}' values were calculated using Bragg equation and average crystallite size calculated of magnesium aluminate nanoparticles by Scherrer equation

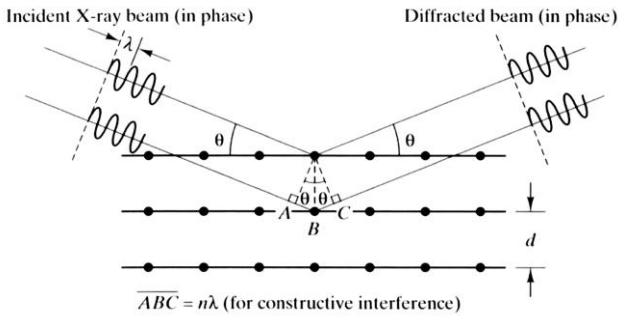

Figure 1 Reflection of crystal planes

$$D = \frac{0.9\lambda}{\beta \cos\theta} \quad (1)$$

where, D is the crystallite size, λ is the wavelength of the X-ray used, β is the full width at half maximum height and θ is the angle of diffraction. Crystals consist of planes of atoms spacing a distance d_{hkl} apart, but can be resolved into many atomic planes, each with a different d_{hkl} spacing.

When there is constructive interference from X-rays scattered by the atomic planes in a crystal, a diffraction peak is observed. The condition for constructive interference from planes with spacing d_{hkl} is given by Bragg's law:

$$\lambda = 2\, d_{hkl} \sin\theta \quad (2)$$

where θ is the angle between the atomic planes and the incident and diffracted X-ray beam. For diffraction to be observed, the detector must be positioned so that the diffraction angle is 2θ, and the crystal must be oriented so that the normal to the diffracting plane is coplanar with the incident and diffracted.

B. Scanning Electron Microscope (SEM)

To observe the morphology of nanocomposites, a Scanning Electron Microscope model JEOL-JSM 5610 LV is used. It is a high-performance, low cost, scanning electron microscope with a high resolution of 3.0 nm. The scanning electron microscope (SEM) is a type of electron microscope that creates various images by focusing a high energy beam of electrons onto the surface of a sample and detecting signals from the interaction of the incident electrons with the sample's surface. The type of signals gathered in a SEM varies and can include secondary electrons, characteristic X-rays, and back scattered electrons. In a SEM, these signals come not only from the primary beam impinging upon the sample, but from other interactions within the sample near the surface. The SEM is capable of producing high-resolution images of a sample surface in its primary use mode, secondary electron imaging. Due to the manner in which this image is created, SEM images have great depth of field yielding a characteristic three-dimensional appearance useful for understanding the surface structure of a sample. This great depth of field and the wide range of magnifications are the most familiar imaging mode for specimens in the SEM. In the SEM, electrons from an electron source are accelerated to high energies and focused through a system of electromagnetic lenses onto the sample. The focused electron beam is scanned across the sample surface, generating different signal as illustrated in Figure 2. Characteristic X-rays are emitted when the primary beam causes the ejection of inner shell electrons from the sample

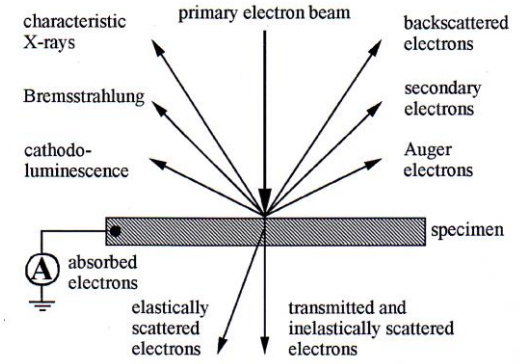

Figure 2 Schematic illustration of the incident electron beam generating different signals in the sample

and are used to tell the elemental composition of the sample. The back-scattered electrons emitted from the sample may be used alone to form an image or in conjunction with the characteristic X-rays as atomic number contrast clues to the elemental composition of the sample.

The SEM provides a highly magnified image of the surface of a material that is very similar to what one would expect if one could actually "see" the surface visually. The resolution of the SEM can approach a few nanometer and it can operate at magnifications that are easily adjusted from about 10X – 300,000X.

In the SEM, a source of electrons is focused (in vacuum) into a fine probe that is rastered over the surface of the specimen. As the electrons penetrate the surface, a number of interactions occur that can result in the emission of electrons or photons from (or through) the surface. A reasonable fraction of the electrons emitted can be collected by appropriate detectors, and the output can be used to modulate the brightness of a cathode ray tube (CRT) whose x- and y-inputs are driven in synchronism with the x-y voltages rastering the electron beam. In this way an image is produced on the CRT; every point that the beam strikes on the sample is mapped directly onto a corresponding point on the screen.

If the amplitude of the saw-tooth voltage applied to the x- and y-deflection amplifiers in the SEM is reduced by some factor while the CRT saw-tooth voltage is kept fixed at the level necessary to produce a full screen display, the magnification, as viewed on the screen, will be increased by the same factor.

III. Sample Preparation

Analytical grade magnesium hydroxide $Mg(OH)_2$ and aluminium oxide Al_2O_3 were used to prepare magnesium aluminate spinel nanoparticles with stoichiometric ($Mg(OH)_2$: Al_2O_3 = 1:1.7) ratios. The amount of $Mg(OH)_2$ and Al_2O_3 powders were accurately weighed and thoroughly mixed in an agate mortar. The mixture was ground to get homogeneous fine powders by using agate mortar and pestle for one and half hours. After that the powders were put in three crucibles to calcinate in electrical furnace. Each crucible containing sample was heated about 700 ˚C, 800 ˚C and 900 ˚C for 1 hr separately. After calcination the samples were ground again for 1 hr to obtain homogeneous powders. Then, these samples were investigated by using XRD and SEM for their structural and morphological properties. Figure 3 showed sample preparation flow chart. The preparation procedures were described in Figures 3 to 8.

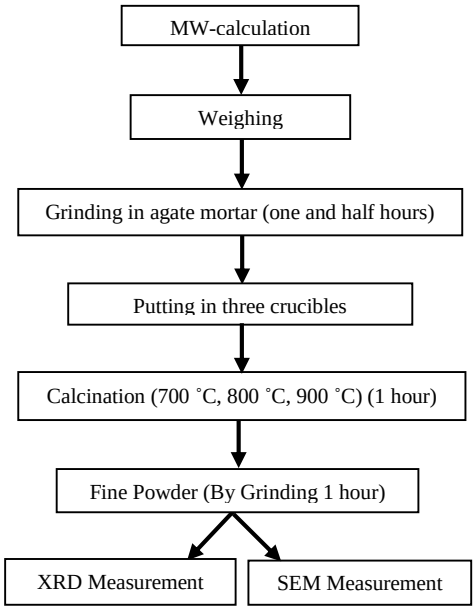

Figure 3 Sample preparation flow chart

(a) (b)

Figure 4 Weighing (a) Al_2O_3 and (b) $Mg(OH)_2$ with digital balance

Figure 5 Grinding two samples with agate mortar and pestle

Figure 6 Ground mixtures with crucibles before calcination

Figure 7 Calcination in electrical furnace at 800 ˚C for 1 hr

Figure 8 Coating for SEM measurement

IV. Results and Discussion

Figure 9 showed the XRD pattern for $MgAl_2O_4$ at 700 ˚C for 1 hr in electrical furnace. The XRD pattern of $MgAl_2O_4$ was analyzed by using JADE software to get the structural properties and crystallite sizes. Study of this figure revealed that the as synthesized sample did not reach the target result. Comparison with the standard cards expressed that some diffraction peaks belonged to $MgAl_2O_4$ (JCPDS 77–1193) while Al_2O_3 (JCPDS 81–2267) and MgO (JCPDS 87–0652) were present as different phase in all the three mixtures. Quantitative analysis done on these diffractograms appeared that the amount of $MgAl_2O_4$ formed at this stage was about 20% with about 45% of Al_2O_3 and remaining 35% of MgO.

The reflection peaks corresponded to the characteristic inter-planar spacing between (1 1 1), (2 2 0), (3 1 1),(4 0 0), (4 2 2), (5 1 1) and (4 4 0) planes of the $MgAl_2O_4$ with a cubic symmetry. According to Table I, the average crystallite size of $MgAl_2O_4$ was 52.08 nm analyzed by XRD data and 38.50 nm calculated by Scherrer equation. The average lattice parameter was 8.0921 Å.

Figure 10 described the XRD pattern for $MgAl_2O_4$ calcined at 800 ˚C for 1 hr in electrical furnace. According to this figure, the as synthesized sample reached the target result. XRD patterns contained no secondary peaks, and therefore the sample had pure structure. From Table II, the average crystallite size of $MgAl_2O_4$ was 16.40 nm determined by XRD data and 16.10 nm calculated by Scherrer equation. The average lattice parameter was 8.0797 Å.

Figure 11 was the XRD pattern for $MgAl_2O_4$ calcined at 900 ˚C for 1 hr in electrical furnace. According to this figure, the as synthesized sample reached the target result. XRD patterns contained no secondary peaks, and therefore the sample had pure structure. By Table III, the average crystallite size of $MgAl_2O_4$ was 31.40 nm determined by

XRD data and 27.93 nm calculated by Scherrer equation. The average lattice parameter was 8.0887 Å.

Table IV showed the comparison of average crystallite sizes of the synthesized samples according to the various calcination temperatures. It was clear that the average crystallite size of $MgAl_2O_4$ at 800 ˚C was the smallest value confirmed by both XRD information and calculation by using Scherrer's equation. Therefore, the powder sample $MgAl_2O_4$ at 800 ˚C should be used to get high performance device such as a refractory in lining of steel-making furnaces, transition and burning zones of cement rotary kilns, checker work of the glass furnace regenerators, sidewalls and bottom of the steel ladles, glass furnaces and melting tanks.

SEM images gave information about the intergranular and intragranular pores as well as the sub-structural defects within the grains. Average grain size was determined using line intercept method. All samples were characterized by small grain and porosity in the as prepared samples was also determined. At 700 ˚C the grain sizes varied from 5 to 6 µm. The surface morphology of $MgAl_2O_4$ (calcined at 800 ˚C) sample as seen from the SEM photographs consisted of grain size varying from 1 to 2 µm and it was the most uniform in grain size among the other samples. In 900 ˚C, the grain sizes were changing from 4 to 5 µm. So, it could be concluded that the smallest grain size was reached at the temperature 800 ˚C.

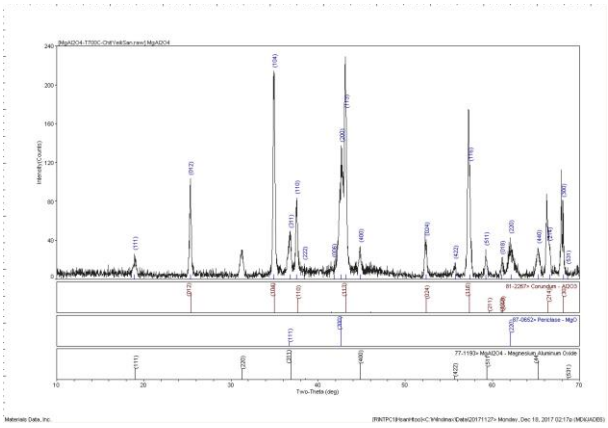

Figure 9 The XRD pattern for $MgAl_2O_4$ calcined at 700 ˚C for 1 hr

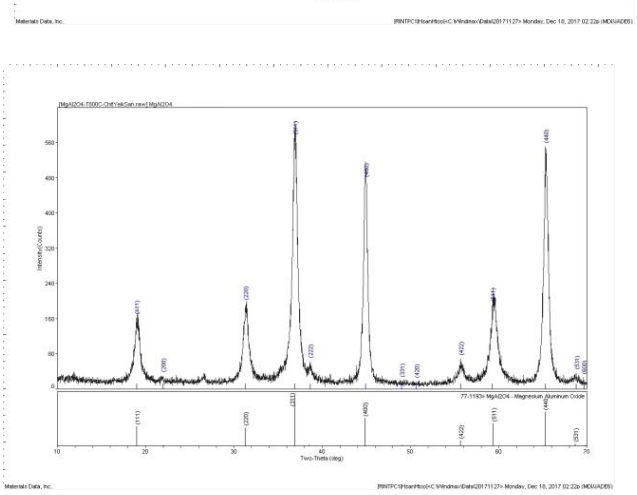

Figure 10 The XRD pattern for $MgAl_2O_4$ calcined at 800 ˚C for 1 hr

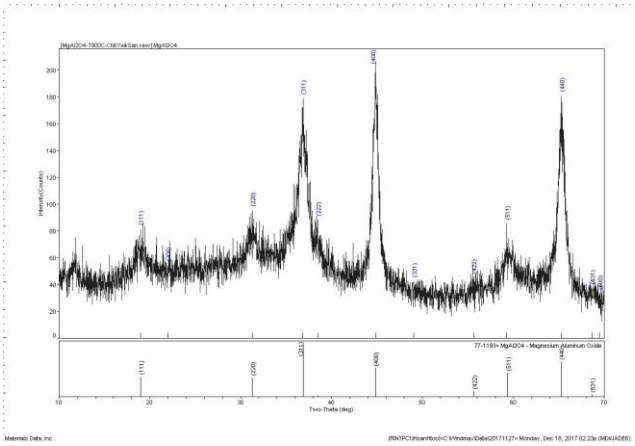

Figure 11 The XRD pattern for $MgAl_2O_4$ calcined at 900 ˚C for 1 hr

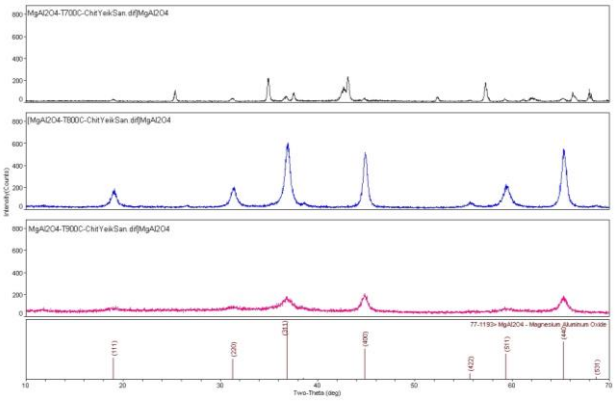

Figure 12 Peaks comparison for $MgAl_2O_4$ at 700 ˚C, 800 ˚C and 900 ˚C for 1 hr

TABLE I. PEAK SEARCH REPORT FOR $MgAl_2O_4$ AT 700 ˚C FOR 1 HR

2θ(˚)	d_{hkl} (Å)	(h k l)	FWHM (˚)	XS(nm)	
				By XRD	*By Calculation*
18.956	4.6777	(1 1 1)	0.264	32.90	30.51
36.809	2.4397	(3 1 1)	0.309	28.60	27.10
38.408	2.3418	(2 2 2)	0.346	>100.0	24.31
44.480	2.0196	(4 0 0)	0.242	39.00	35.47
55.743	1.6477	(4 2 2)	0.194	54.20	46.32
59.258	1.5581	(5 1 1)	0.107	>100.0	85.41
65.270	1.4283	(4 4 0)	0.359	27.30	26.28
68.642	1.3662	(5 3 1)	0.295	34.60	32.61
Average crystallite size				52.08	38.50

TABLE II. PEAK SEARCH REPORT FOR $MgAl_2O_4$ AT 800 ˚C FOR 1 HR

2θ(˚)	d_{hkl} (Å)	(h k l)	FWHM (˚)	XS(nm)	
				By XRD	*By Calculation*
18.962	4.6764	(1 1 1)	0.552	14.80	14.59
31.294	2.8559	(2 2 0)	0.577	14.50	14.30
36.881	2.4351	(3 1 1)	0.605	14.00	13.84
38.633	2.3286	(2 2 2)	0.452	19.10	18.62
44.904	2.0169	(4 0 0)	0.516	17.00	16.66
55.685	1.6493	(4 2 2)	0.441	20.90	20.37
59.276	1.5576	(5 1 1)	0.710	13.00	12.87
65.300	1.4278	(4 4 0)	0.537	17.90	17.57
Average crystallite size				16.40	16.10

TABLE III. PEAK SEARCH REPORT FOR $MgAl_2O_4$ AT 900 ˚C FOR 1 HR

2θ(˚)	d_{hkl}(Å)	(h k l)	FWHM (˚)	XS(nm)	
				By XRD	*By Calculation*
18.958	4.6773	(1 1 1)	0.485	17.00	16.61
31.290	2.8563	(2 2 0)	0.345	25.00	23.91
36.845	2.4374	(3 1 1)	0.611	13.90	13.70
38.466	2.3384	(2 2 2)	0.108	>100.0	77.91
44.847	2.0194	(4 0 0)	0.496	17.70	17.33
55.623	1.6510	(4 2 2)	0.272	35.50	33.02
59.252	1.5582	(5 1 1)	0.373	25.40	24.50
65.286	1.4280	(4 4 0)	0.573	16.70	16.47
Average crystallite size				31.40	27.93

TABLE IV. COMPARISON FOR AVERAGE CRYSTALLITE SIZES OF $MgAl_2O_4$ AT 700 ˚C, 800 ˚C AND 900 ˚C FOR 1 HR

Calcination Temperature	XS(nm)	
	By XRD	*By Calculation*
Average crystallite size at 700 ˚C (1 hr)	52.08	38.50
Average crystallite size at 800 ˚C (1 hr)	16.40	16.10
Average crystallite size at 900 ˚C (1 hr)	31.40	27.93

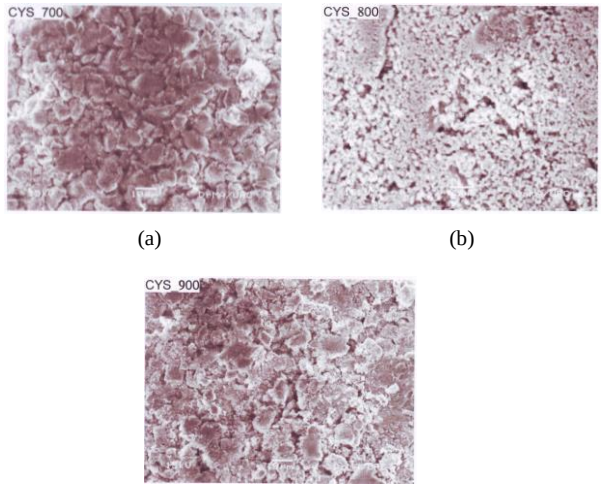

(a) (b)

(c)

Figure 13 SEM images of $MgAl_2O_4$ calcined at (a) 700 ˚C (b) 800 ˚C and (c) 900 ˚C for 1 hr

V. CONCLUSION

Quantitative conversion of MgO - Al_2O_3 mixtures into high purity $MgAl_2O_4$ using the high temperature melting characteristics of metallic aluminum has been demonstrated. The precursor mixture was crushed into powder and calcinated at temperatures 700 ℃, 800 ℃ and 900 ℃ for 1 hour. XRD and SEM techniques were used for characterization of the product. The crystallite size and lattice constant of $MgAl_2O_4$ nano- particles were calculated depending upon the data of X-ray. X-ray diffraction analysis clearly revealed that all the particles have the structure cubic spinel. According to XRD data, the average crystallite size of $MgAl_2O_4$ at 800 ˚C was the smallest value about 16.40 nm and 16.10 nm. Surface morphologies of spinel samples were investigated by using SEM. From these figures, it was clear that the grain size of $MgAl_2O_4$ sample at temperature 800 ˚C was the smallest size among three samples. One of the limitations of SHS synthesis was the presence of relatively high degree of porosity in the material. The powder sample $MgAl_2O_4$ at 800 ˚C was the most uniform in grain size among the other samples. Therefore, it was concluded that the powder sample ($MgAl_2O_4$ at 800 ˚C) should be used to get high performance device such as infrared and humidity sensors, armour materials, excellent transparent material for arc-enclosing envelopes and alkali-metal vapour discharge devices.

ACKNOWLEDGMENT

We would like to thank Pro-Rector Dr Khin Maung Chin, Technological University (Yamethin), for his kind permission to accept this research work. We also thank reviewers from Technological University (Yamethin) for this research paper. Thanks are also due to our colleagues for their valuable advice and collaboration on this research.

REFERENCES

[1] Ei Zar Tun, “Structural and Surface Morphology of Mg-Cu Ferrite Material”, MRes Thesis: Taungoo University, 2017.

[2] L. R. Ping, A. M. Azad and T. W. Dung, “Magnesium aluminate ($MgAl_2O_4$) spinel produced via self-heat-sustained (SHS) technique”, *Materials Research Bulletin*, vol. 36, pp. 1417-1430, 2001.

[3] Wut Yi Nway, “Structural and Surface Morphology of $MgFe_2O_4$ Ferrite Material”, MRes Thesis: Taungoo University, 2016.